Reversible electrochemistry of fumarate reductase immobilized on an electrode surface. Direct voltammetric observations of redox centers and their participation in rapid catalytic...

ARTICLE *in* BIOCHEMISTRY · JUNE 1993

Impact Factor: 3.02 · DOI: 10.1021/bi00071a023 · Source: PubMed

4 AUTHORS, INCLUDING:

Richard Cammack
King's College London
345 PUBLICATIONS **8,676** CITATIONS
SEE PROFILE

Joel H Weiner
University of Alberta
191 PUBLICATIONS **6,830** CITATIONS
SEE PROFILE

Reversible Electrochemistry of Fumarate Reductase Immobilized on an Electrode Surface. Direct Voltammetric Observations of Redox Centers and Their Participation in Rapid Catalytic Electron Transport†

Artur Sucheta,‡ Richard Cammack,§ Joel Weiner,‖ and Fraser A. Armstrong*,‡

Department of Chemistry, University of California, Irvine, California 92717, Division of Biomolecular Sciences, King's College London, Campden Hill Road, London W8 7AH, United Kingdom, and Department of Biochemistry, University of Alberta, Edmonton, Alberta, Canada T6G 2H7

Received December 15, 1992; Revised Manuscript Received February 26, 1993

ABSTRACT: Fumarate reductase (*Escherichia coli*) can be immobilized in an extremely electroactive state at an electrode, with retention of native catalytic properties. The membrane-extrinsic FrdAB component adsorbs to monolayer coverage at edge-oriented pyrolytic graphite and catalyzes reduction of fumarate or oxidation of succinate, depending upon the electrode potential. In the absence of substrates, reversible redox transformations of centers in the enzyme are observed by cyclic voltammetry. The major component of the voltammograms is a pair of narrow reduction and oxidation signals corresponding to a pH-sensitive couple with formal reduction potential $E^{\circ\prime}$ = –48 mV vs SHE at pH 7.0 (25 °C). This is assigned to two-electron reduction and oxidation of the active-site FAD. A redox couple with $E^{\circ\prime}$ = –311 mV at pH 7 is assigned to center 2 ([4Fe-4S]$^{2+/1+}$). Voltammograms for fumarate reduction at 25 °C, measured with a rotating-disk electrode, show high catalytic activity without the low-potential switch-off that is observed for the related enzyme succinate dehydrogenase. The catalytic electrochemistry is interpreted in terms of a basic model incorporating mass transport of substrate, interfacial electron transfer, and intrinsic kinetic properties of the enzyme, each of these becoming a rate-determining factor under certain conditions. Electrochemical reversibility is approached under conditions of low turnover rate, for example, as the supply of substrate to the active site is limited. In this situation, electrocatalytic half-wave potentials, $E_{1/2}$, are similar for oxidation of bulk succinate and reduction of bulk fumarate and coincide closely with the $E^{\circ\prime}$ value assigned to the FAD. At 25 °C and pH 7, the apparent K_M for fumarate reduction is 0.16 mM, and k_{cat} is 840 s^{-1}. Accordingly the second-order rate constant, k_{cat}/K_M, is 5.3 × 10^6 M^{-1} s^{-1}. Under the same conditions, oxidation of succinate is much slower. As the supply of fumarate to the enzyme is raised to increase turnover, the electrochemical reaction eventually becomes limited by the rate of electron transfer from the electrode. Under these conditions a second catalytic wave becomes evident, the $E_{1/2}$ value of which corresponds to the reduction potential of the redox couple suggested to be center 2. This small boost to the catalytic current indicates that the low-potential [4Fe-4S] cluster can function as a second center for relaying electrons to the FAD.

Biological[5] interconversion of fumarate and succinate is catalyzed by oxidoreductases known as fumarate reductase (FRD) and succinate dehydrogenase (SDH) (Cole et al., 1985; Ohnishi, 1987; Ackrell et al., 1992). These closely related enzymes exist as membrane-bound complexes, respectively menaquinol:fumarate oxidoreductase and succinate:ubiquinone oxidoreductase (also known as complex II), that link oxidation of succinate or reduction of fumarate to reduction or oxidation of the quinone pool (Q/QH_2) as shown by eq 1.

$$\text{fumarate} + QH_2 \rightleftharpoons \text{succinate} + Q \qquad (1)$$

In *Escherichia coli* and other bacteria, fumarate can serve as a terminal electron acceptor in anaerobic respiration (Haddock & Jones, 1977; Ingledew & Poole, 1984). The FRD complex is located in the cytoplasmic membrane and comprises four nonidentical subunits organized into two domains (Ackrell et al., 1992). The four genes encoding these subunits have been cloned and sequenced, and FRD now provides an important model system for studying active-site structure and function in complex respiratory enzymes (Blaut et al., 1989; Westenberg et al., 1990; Schröder et al., 1991; Werth et al., 1990, 1992).

The soluble membrane-extrinsic "catalytic" domain of FRD consists of subunit FrdA (66 kDa), which contains a covalently bound FAD (Weiner & Dickie, 1979; Blaut et al., 1989) and the site of substrate binding, and subunit FrdB (27 kDa), which contains the iron–sulfur clusters, centers 1 ([2Fe-2S]$^{2+/1+}$), 2 ([4Fe-4S]$^{2+/1+}$), and 3 ([3Fe-4S]$^{1+/0}$) (Manodori et al., 1992). The reduction potentials of centers 1 and 3 lie in the range –20 to –70 mV appropriate for mediating electron transfer from menaquinol to fumarate (Cammack et al., 1984; Simpkin & Ingledew, 1985; Cammack et al., 1986, 1987; Werth et al., 1990). Conversely, the much more negative reduction potential reported for center 2 (range –285 to –320 mV) poses a problem with regard to its role in the functioning of the enzyme (Simpkin & Ingledew, 1985; Cammack et al., 1986, 1987). The catalytic domain is associated with the membrane via a membrane-intrinsic "anchor" domain consisting of subunits FrdC (15 kDa) and FrdD (13 kDa). These are essential for reaction with menaquinone (Weiner et al.,

† This work was supported by grants from the Donors of the Petroleum Research Fund administered by the American Chemical Society (F.A.A.), by the National Science Foundation (MCB-9118772) (F.A.A.), and by the University of California.

* To whom correspondence should be addressed at the University of California.

‡ University of California.

§ King's College London.

‖ University of Alberta.

0006-2960/93/0432-5455$04.00/0

1986; Westenberg et al., 1990). However, a soluble enzyme consisting only of FrdA and FrdB subunits (FrdAB) can be prepared which is active in fumarate reduction by benzyl viologen (Robinson & Weiner, 1982; Lemire & Weiner, 1986).

Recently it was shown that the analogous, soluble two-subunit form of SDH (bovine heart mitochondria) exhibits direct unmediated catalytic electrochemistry when adsorbed at an edge-oriented pyrolytic graphite electrode (Sucheta et al., 1992). Such voltammetric methods are proving to have increasing applicability for studying redox proteins that have unstable, reactive centers (Armstrong, 1990, 1992; Armstrong et al., 1993a; Butt et al., 1991, 1993). For an *enzyme*, moreover, they permit catalytic performance to be measured under conditions of continuously variable applied potential (Varfolomeev & Berezin, 1978; Hill, 1993). Detailed information may thus be obtained on how activity is linked to the energetics of the catalyzed reaction and to the redox status of active sites. From studies with SDH, it was concluded that the adsorbed enzyme remains fully functional with regard to succinate oxidation. Furthermore, it was found that catalysis in the direction of fumarate reduction (physiologically the reverse process) is controlled by an interesting potential gating effect. Specifically, reduction of fumarate is catalyzed only within a narrow region of applied potential, with activity being "switched off" as the electrochemical driving force is increased. This fully reversible phenomenon has now been observed in nonelectrochemical kinetic experiments with SDH from various sources and intact complex II (Ackrell et al., 1993). These studies have revealed that the rate of oxidation of benzyl viologen radical by fumarate as catalyzed by SDH *increases* with the formation (or addition) of the oxidized product, i.e., opposite to the profile observed with FRD. The physiological relevance of this property is under consideration.

In this paper we describe direct voltammetric experiments on the FrdAB component of fumarate reductase. The results provide (i) an unambiguous demonstration of the capability of an enzyme to exhibit reversible electrocatalysis when bound in a near-monolayer film at an electrode surface, (ii) a voltammetric "snapshot" of active sites and their participation in turnover, and (iii) measurements of kinetic parameters that reveal large rate constants for electron transfer between the electrode and the enzyme and within the enzyme itself. Results are discussed in terms of a generic model capable of wide application in future developments.

EXPERIMENTAL PROCEDURES

The membrane-extrinsic catalytic dimer (FrdAB) of fumarate reductase was isolated from *E. coli* HB101/pFRD84 according to a previously reported method (Lemire & Weiner, 1986). The enzyme was assayed by monitoring oxidation of reduced benzyl viologen by fumarate as described by Dickie and Weiner (1979). The activity of the sample used in these studies was 511 units mg^{-1}. Because of the air sensitivity of soluble FRD, all experiments and preliminary handling of the enzyme were undertaken in a glovebox under an atmosphere of argon or nitrogen (O_2 < 1ppm). Concentrated enzyme solutions were prepared by diafiltration with an Amicon 8MC (YM10 membrane), and the concentration was determined by spectrophotometry using ϵ = 10 mM^{-1} cm^{-1} at 460 nm (Weiner & Dickie, 1979). Purified water of resistivity ~18 MΩ cm was used throughout.

For all electrochemical studies, a supporting electrolyte consisting of 0.1 M NaCl (Aldrich) 50 mM in an appropriate buffer was used. These buffers were TAPS (3-[[tris(hydroxymethyl)methyl]amino]propanesulfonic acid), HEPES (*N*-(2-hydroxyethyl)piperazine-*N'*-2-ethanesulfonic acid), MES (4-morpholineethanesulfonic acid), and PIPES (1,4-piperazinediethanesulfonic acid]), each purchased from Sigma. All buffers were prepared, and their pH was adjusted by addition of concentrated NaOH or HCl as needed, at 25 °C (or 0 °C for low-temperature studies). Polymyxin B sulfate was obtained from Sigma and prepared as a stock solution of about 30 mg/mL with its pH adjusted to 7.0.

For cyclic voltammetry (CV) at stationary and rotating disk electrodes, an Ursar Scientific Instruments (Oxford) potentiostat was used. An EG&G M636 electrode rotator and control unit were used for rotating disk experiments. The all-glass voltammetric cell was similar to that described previously (Armstrong et al., 1989a) except that the sample compartment was equipped with a circulating jacket for thermostatting. The rotating-disk electrode (RDE) was a small cylinder of pyrolytic graphite (Le Carbone, France) cut so that the ends exposed the "edge" plane (hence the term "PGE" for pyrolytic graphite edge) which was mounted in a Teflon sheath enclosing a brass contact rod. The sheath was machined for compatibility with the cell and featured a ferrule equipped with a grub screw for rapid attachment to the electrode rotator. Prior to each experiment, the electrode was polished with an aqueous slurry of 0.3-μm alumina (Buehler micropolish) and sonicated thoroughly. A Fisher saturated calomel electrode (SCE) was used as the reference. All potentials given are with reference to the standard hydrogen electrode (SHE); our values are based on $E°'$(SCE) = 0.241 V (Bard & Faulkner, 1980). The auxilliary electrode was a piece of platinum gauze.

All aspects of the rotating-disk system (cell, electrode, potentiostat) were checked by conducting experiments at 25 °C with solutions of $Fe(CN)_6^{3-}$ containing 0.1 M NaCl and 50 mM PIPES, pH 7. Data yielded Levich plots (Levich, 1944; Riddiford, 1966) that were linear up to a rotation rate of at least 1800 rpm. Tests were performed under conditions in which the limiting current, i_{lim}, exceeded values observed in experiments with fumarate reductase. It was confirmed that the current–potential (i–E) curves for reduction of $Fe(CN)_6^{3-}$ were symmetrical about the half-wave potential and gave linear plots (slope 59 mV) of E against $\log\{(i_{lim} - i)/i\}$ (Bond, 1980; Bard & Faulkner, 1980; Southampton Electrochemistry Group, 1985). Levich plots (i_{lim} vs square root of rotation rate) had slopes directly proportional to the bulk concentration of ferricyanide, with the proportionality coefficient given by $0.620FAD^{2/3}\nu^{-1/6}$ (see eq 4 and definitions given below); this relationship was used to determine the electroactive surface area of the electrodes. Values of ν and D were taken to be 0.01 cm^2 sec^{-1} and 0.763 × 10^{-5} cm^2 sec^{-1}, respectively (Bard & Faulkner, 1980; Adams, 1969).

The electrochemistry of FRD was enhanced and stabilized in the presence of polymyxin and (to a lesser extent) neomycin, which we have previously shown to induce strong adsorption of ferredoxins at a PGE electrode (Armstrong et al., 1989, 1993a; Butt et al., 1991, 1993). Unless otherwise stated, all experiments were performed with electrolyte solutions containing 0.1–1.0 g L^{-1} (0.08–0.75 mM) polymyxin B sulfate (Hayashi & Suzuki, 1965) which was added as an aliquot of the concentrated stock solution.

RESULTS AND DISCUSSION

Detection, Optimization, and a Preliminary Description of the Catalytic Electrochemistry as Measured at a Stationary Electrode. Following introduction of a freshly polished electrode into a solution containing fumarate and 0.3 μM

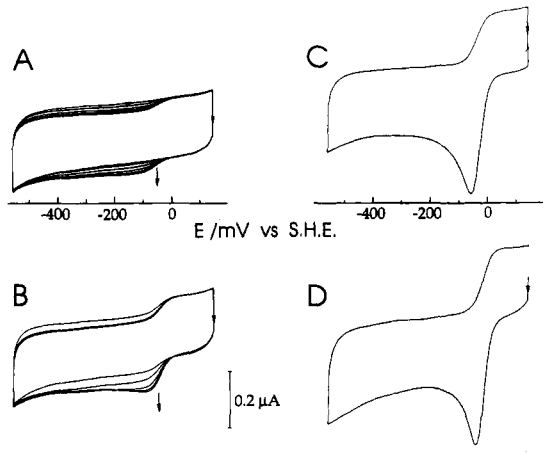

FIGURE 1: Cyclic voltammograms measured with a stationary PGE electrode on successive cycles following introduction of the electrode into a solution containing 25 μM fumarate and 0.10 M NaCl at 25 °C and pH 7.0 (PIPES). Electrode surface area is 0.09 cm^2; scan rate, 9.7 mV s^{-1}. (A) Successive cycles in solution containing 0.33 μM fumarate reductase (FrdAB) and no polymyxin. (B) Successive cycles in solution containing 0.33 μM FrdAB and 0.1 g/L polymyxin. (C) Single cycle following a potential hold for 2 min at −160 mV; 0.82 μM FrdAB, no polymyxin. (D) Single cycle following a potential hold for 2 min at −160 mV; 0.82 μM FrdAB, 0.1 g/L polymyxin.

FrdAB, a sigmoidal reduction wave develops upon repetitive cycling over the potential range 150 to −550 mV. This is shown in Figure 1A. The size of the wave increases as the fumarate concentration is raised (in this case the concentration is 25 μM) but decreases very markedly as the temperature is lowered from 25 to 0 °C. No faradaic response in this region is observed for a solution of fumarate without the enzyme. These observations are consistent with enzymatic catalysis of the electrochemically driven reduction of fumarate. After a period of time the response deteriorates, even after brief stirring of the solution to replenish the substrate close to the electrode. As shown in Figure 1B, if the same experiment is carried out in the presence of polymyxin, a more rapid and marked development is observed, with the response changing from a sigmoidal wave to a peak. The stability of the optimal response is also considerably greater. Increases in the enzyme concentration (up to 0.8 μM) produce a much sharper, peak-like response in a shorter time.

If the electrode, at the point of attaining the maximal response, is rinsed with buffer and then transferred to a solution containing all the components except fumarate reductase, electrocatalytic activity remains detectable for at least 15 min. During this time the response reverts to the sigmoidal waveform; however, the attenuation occurs more rapidly than the deterioration observed when enzyme is present in the solution. These observations show that FrdAB is reversibly adsorbed at the electrode surface. The transition from sigmoidal to peak-type catalytic waveform therefore reflects the progress of adsorption, with the optimal peak-type response being associated with the highest coverage of active enzyme molecules. Such a time dependence resembles the observation made for electrocatalysis of H_2O_2 reduction by cytochrome *c* peroxidase (Armstrong & Lannon, 1987; Armstrong et al., 1993b).

Several factors were investigated in order to establish conditions for reproducibly obtaining optimal results. We adopted a working hypothesis to gauge optimization: for a given substrate concentration, maximum coverage of active enzyme is associated with the most positive peak potential and highest peak current (Armstrong et al., 1993b). For pH 7, it was found that this condition could be achieved with an enzyme concentration of 0.8 μM and a polymyxin concentration of 0.1 g L^{-1}. The influence of the applied potential upon the adsorption process was assessed by poising the immersed electrode at various potentials for different times before initiating scanning. In this way it was ascertained that a value of −160 mV gave reproducibly good results. Panels C and D of Figure 1 show voltammograms obtained after holding the potential at −160 mV for 2 min prior to scanning. For Figure 1C, polymyxin is absent, whereas it is present at a concentration of 0.1 g L^{-1} for the experiment shown in Figure 1D. Solution conditions are the same as for Figure 1A,B except that the enzyme concentration is 0.8 μM. Close inspection shows that the peak potential is more positive in Figure 1D (−40 mV) than in Figure 1C (−59 mV); moreover, the voltammogram was much more stable over successive scans. The observations that the response is both sharpened and stabilized in the presence of polymyxin indicate that its likely role is either to promote adsorption of active enzyme molecules in such a manner that denaturation is retarded (e.g., by participating in the enzyme–electrode assembly) or to prevent adsorption of inactive molecules that would otherwise block the electrode surface.

Similar results were obtained over the pH range 7–9, but at pH 6 a much higher level of polymyxin, e.g., 1 g L^{-1}, was required to give a stable response. Neomycin also was found to promote enzyme adsorption. In studies with ferredoxins, we have found that reagents such as polymyxin or neomycin induce formation of films close to monolayer coverage that are stable for extended periods in the absence of a bulk concentration of the protein (Armstrong, 1992; Armstrong et al., 1989b, 1993a; Butt et al., 1991, 1993).

By contrast with the characteristic voltammetry observed for the case of succinate dehydrogenase (Sucheta et al., 1992), there is no evidence for potential-controlled gating of the reduction of fumarate. The reduction peak that is observed upon scanning in the direction of decreasing potential is as expected for a reaction controlled by diffusion of a reducible substrate to a planar electrode surface (Nicholson & Shain, 1964; Bard & Faulkner 1980). That this peak arises from depletion of the diffusion layer by extremely efficient catalysis is demonstrated by the fact that it transforms to a large sigmoidal wave upon rotating the electrode. For satisfactory data analysis and interpretation it was thus essential to achieve strict control over mass transport of substrate, and further studies of the electrocatalytic reaction were carried out with a rotating disk electrode.

Demonstration of Electrochemically Near-Reversible Catalysis by FRD Using a Rotating Disk Electrode. Figure 2 shows RDE voltammograms (*i*–*E* curves) obtained at 25 °C for solutions of fumarate reductase (0.1 M NaCl and 20 mM PIPES at pH 7.0) in the presence of low levels of substrate, respectively 2.6 μM fumarate or 13 μM succinate. In each case, scanning was performed after inducing optimal activity by poising the potential at −160 mV for 2 min. As the applied potential, *E*, is varied in the direction required to cause reduction of succinate or oxidation of fumarate (in this case at a scan rate (v) of 9.7 mV s^{-1}), the faradaic current, *i*, increases, finally reaching a constant value, i_{lim}, at which it is clear that the electrochemical potential ceases to be a factor controlling the current. Upon changing the direction of scanning, the same curves are traced with the current offset by the double-layer capacitance (the magnitude of which depends directly upon the scan rate). Compared to background voltammograms measured in the absence of substrate, fumarate caused a negative displacement of the current, while

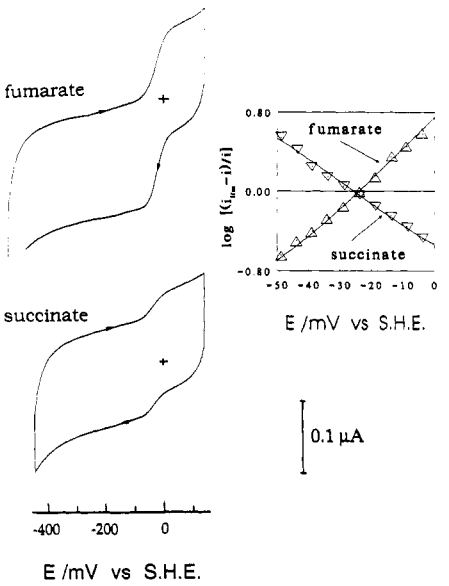

FIGURE 2: Cyclic voltammograms demonstrating the reversibility of electrochemical turnover of fumarate or succinate by fumarate reductase adsorbed at a rotating PGE disk electrode. Scans shown were recorded after development of maximum activity at 25 °C. The respective origins of the current–potential coordinate systems are marked by a cross. Conditions: 1.2 μM FrdAB; 0.46 g/L polymyxin; 20 mM PIPES at pH 7; 0.1 M NaCl; temperature, 25 °C; scan rate, 9.7 mV s^{-1}. For fumarate (2.6 μM) the electrode rotation rate is 300 rpm. For succinate (13 μM) the rotation rate is 900 rpm. The insert shows plots of $\log(i_{lim} - i)/i$ (∇, succinate oxidation; Δ, fumarate reduction) against applied potential, E, for scans in direction of increasing potential.

succinate caused a positive displacement, thus confirming the electrode reactions as reduction and oxidation, respectively. The forms of the faradaic component of the corresponding i–E curves obtained at a slower scan rate (4.9 mV s^{-1}) were identical within experimental error.

For reversible electrochemistry with a solution comprising oxidant O under steady-state conditions (as approached through a technique such as RDE voltammetry or polarography) the relationship between current and potential is given by the Heyrovský–Ilković equation (Heyrovský & Kůta, 1966; Bond, 1980; Bard & Faulkner, 1980; Southampton Electrochemistry Group, 1985). In the specific case of a simple, noncatalytic, diffusion-controlled reaction, this equation can be written as

$$E = E_{1/2} + (2.3RT/nF) \log\{(i_{lim} - i)/i\} \qquad (2)$$

Provided reactant O and product R have equal diffusion coefficients, the "half-wave" potential, $E_{1/2}$ coincides with the formal reduction potential, $E^{\circ\prime}$, of the O/R couple. Equation 2 predicts that a plot of $\log\{(i_{lim} - i)/i\}$ against E should be a straight line of reciprocal slope $2.3RT/nF$ intercepting the potential axis at $E_{1/2}$. The term n in this case reflects the stoichiometry of the reaction. The same value of $E_{1/2}$ is expected if the experiment is carried out in the reverse direction, i.e., oxidizing the bulk reductant R.

The inset to Figure 2 shows the corresponding plots of $\log\{(i_{lim} - i)/i\}$ (corrected for background slope) against E. These are approximately linear, with slopes of 30–45 mV per decade, and yield $E_{1/2}$ values that are in close agreement with each other. At pH 7.0 and 25 °C, $E_{1/2}$ is -32 ± 5 for fumarate reduction and -26 ± 5 mV for succinate oxidation. For experiments with fumarate, elevated substrate concentrations or higher electrode rotation rates gave increasing distortion of the voltammogram toward the low-potential limit. This

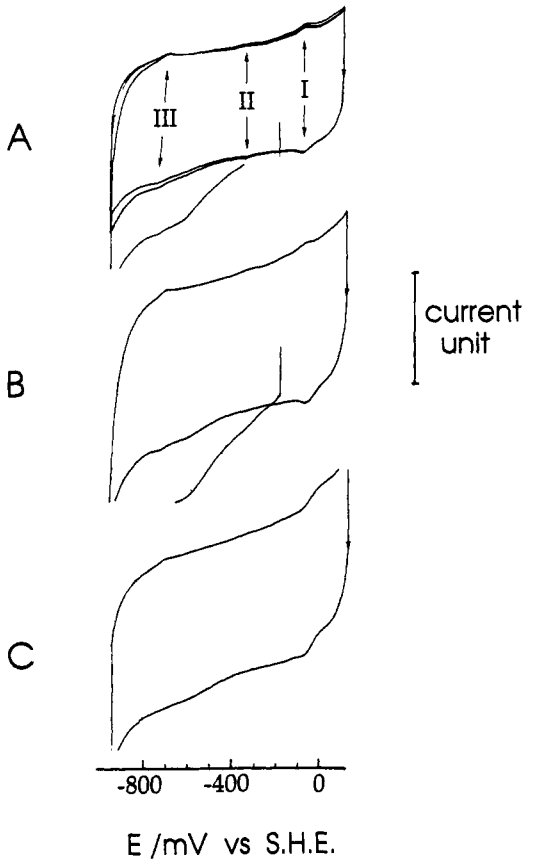

FIGURE 3: Voltammograms of a solution containing 0.82 μM FrdAB, 0.1 g/L polymyxin, and 0.10 M NaCl at pH 7.0 (PIPES) and 25 °C. Electrode surface area is 0.09 cm^2. (A) Successive cycles at a stationary electrode (scan rate, 50 mV s^{-1}, current unit, 10 μA) following a potential hold for 2 min at –160 mV. The positions of signals I, II, and III are indicated. The initial cycle exhibits an additional broad current component in the direction of decreasing potential due to irreversible reduction of electrode surface groups. (B) Voltammogram recorded in the presence of 0.4 μM fumarate a stationary electrode following a potential hold at –160 mV and brief rotation of the electrode (scan rate, 10 mV s^{-1}; current unit, 0.2 μA). (C) Voltammogram recorded in the presence of 0.4 μM fumarate with an electrode rotation rate of 1200 rpm following a potential hold for 2 min at –160 mV (scan rate, 10 mV s^{-1}; current unit, 0.2 μA).

observation (which we propose arises as turnover becomes limited by the rate of electron transfer to the enzyme from the electrode) is discussed later.

We thus conclude that, under low rates of turnover, the voltammetric response conforms to some of the basic expectations for a reversible electrode reaction. However, three observations reflect the controlling influence of the enzyme. First, the current obtained per concentration unit of succinate is much lower than for fumarate (n.b., the diffusion coefficients of succinate and fumarate should be similar). Second, the $E_{1/2}$ value observed is more negative (by approximately 60 mV) than the reported reduction potential $E^{\circ\prime}_{F/S}$ (30 mV) for the fumarate–succinate redox couple under similar conditions (Clark, 1960). Third, the n values are below the value of 2.0 expected for equilibrium between fumarate and succinate.

Detection of Reversible, Noncatalytic Electron Exchange between the Electrode and the Redox Centers of Adsorbed Enzyme Molecules. A cyclic voltammogram of an enzyme solution at 25 °C recorded in the absence of fumarate is shown in Figure 3A. Several isolated pairs of oxidation and reduction waves are observed following immersion of a freshly polished electrode and poising of the potential initially at –160 mV for 2 min prior to cycling. The peaks are easily visible above the

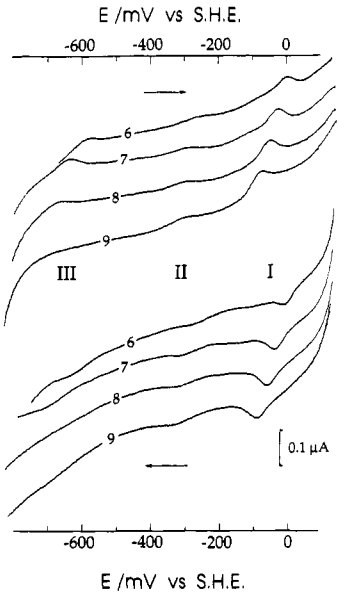

FIGURE 4: Stationary-electrode cyclic voltammograms of solutions containing 0.82 μM FrdAB and 0.10 M NaCl at 0 °C. No fumarate was present in solutions. Electrode surface area is 0.09 cm²; scan rate, 50 mV s⁻¹. Voltammograms were recorded after a potential hold for 2 min at −160 mV. Conditions: pH 6 (6.0), pH 7 (7.0), pH 8 (8.0), and pH 9 (9.1).

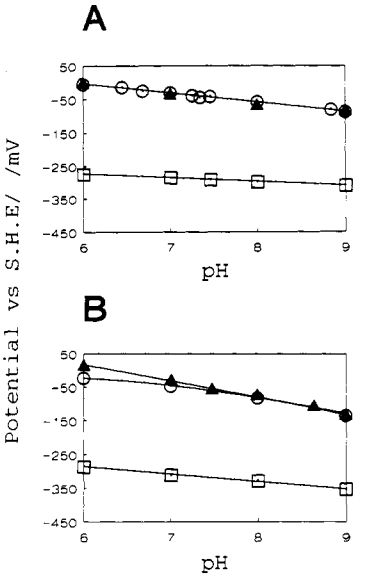

FIGURE 5: Graph showing the variation of $E^{\circ\prime}_{I}$ (○) and $E^{\circ\prime}_{II}$ (□) with pH for fumarate reductase adsorbed at PGE electrodes at 0 °C (A) and 25 °C (B). Other conditions are as for Figure 4. Graphs also show the positions of $E_{1/2}$ (▲) observed for reduction of low concentrations of fumarate. Low-temperature $E_{1/2}$ values are for 3 °C. Errors are ±5 mV for $E^{\circ\prime}_{I}$ and $E_{1/2}$, and ±10 mV for $E^{\circ\prime}_{II}$.

large but relatively uniform background from double-layer capacitance. The amplitudes of three pairs of such peaks, which we shall refer to as signals I, II, and III in order of decreasing potential, diminish slowly with time coincidentally with the appearance of a weak, broad feature in the region of −150 to −200 mV, and on the same time scale as the decrease in catalytic activity mentioned above. Signal I is the most prominent feature, with oxidation and reduction peaks being of equal size and coinciding in potential position to within 25 mV even at a scan rate of 470 mV s⁻¹. Signal II is less pronounced and noticeably broader although oxidation and reduction peaks have similar shapes and again appear of equal size. On the other hand, signal III clearly arises from a complicated redox process since the reduction wave is broader than the oxidation wave, and this asymmetry is particularly marked at high scan rate. Importantly, the entire voltammogram is unchanged upon rotation of the electrode. We thus conclude that the signals arise from sites in molecules that are confined to the electrode surface and for which diffusional exchange with bulk solution is negligible during the time course of the scan. The formal reduction potentials of signals I and II are −48 ± 5 and −311 ± 10 mV, respectively, as determined from the average of oxidation and reduction peak potentials. We did not attempt to determine a value for signal III because of the apparent complexity of its dependence on experimental parameters.

Addition of fumarate to a final concentration even as low as 0.4 μM produces marked changes in the voltammetry. Examined with a stationary electrode (as shown in Figure 3B), the reduction peak of signal I is enlarged. Little change occurs elsewhere. However, upon rotating the electrode (Figure 3C), both the reduction and oxidation peaks of signal I vanish entirely to be replaced by a sigmoidal wave, the form and position of which ($E_{1/2}$ = −31 mV, n = 1.7–1.8) agree with the result observed with the severalfold higher fumarate concentration described above. Each of the other signals (as well as the redox couple in the region of −200 mV that eventually dominates at longer times) remain peak-like, although signal II appears attenuated compared to the zero-substrate/zero-rotation experiment. These results specifically identify the entire population of centers giving rise to signal I as being directly involved in catalytic electron transport and indicate a high catalytic rate constant for the adsorbed enzyme.

Figure 4 shows cyclic voltammograms recorded for enzyme solutions over a range of pH at 0 °C, in the absence of fumarate or succinate. As before, these were recorded after the potential was initially poised at −160 mV for 2 min to develop maximum signal size. For pH 6, a greater concentration of polymyxin was required to provide stability, and the current peaks were consistently of somewhat lower amplitude. Generally, however, the peaks are sharper and permit more detailed examination compared to the results obtained at 25 °C. Voltammograms were stable for a period of at least 20 min. Peak currents were proportional to scan rate, although we again observed that the waves of signal III are broadened at high scan rate, with the effect being particularly marked for the reduction component.

From the following considerations, we conclude that signal I arises from a redox couple involving concerted transfer of more than one electron. Theory predicts that the voltammetric response arising from reversible electrochemistry of an "ideal", non-interacting, homogeneous population of diffusionless redox couples should consist of reduction and oxidation peaks that are symmetrical about the formal reduction potential, $E^{\circ\prime}$, and have a half-height width, δ, of $3.52RT/nF$ volts ($83/n$ mV at 0 °C) (Laviron, 1979a,b). Even though the baseline of these peaks cannot be determined with certainty (and we believe, as mentioned below, that they must overlay two much broader signals from centers 1 and 3), it is clear that δ must be considerably less than 83 mV. Adopting a reasonable baseline by inspection, we estimate that δ is in the order of 50 mV or less. Since environmental heterogeneity must serve only to increase δ, and considering that interactions between like centers in adjacent macromolecules are extremely unlikely (by contrast with the case for small adsorbed molecules), we conclude that n must lie close to 2 (Laviron, 1979a). The pH dependence of the formal reduction potential, $E^{\circ\prime}_{I}$, at 0 °C is shown in Figure 5A, and data are displayed in Table I. The plot is linear with a gradient of −29 mV/pH unit, thu

Table I: Formal Reduction Potentials ($E^{\circ\prime} = \{E_{pa} - E_{pc}\}/2$) for Redox Couples Observed in the Absence of Fumarate and Half-Wave Potentials ($E_{1/2}$) Observed for Catalysis under Conditions of Low Fumarate Concentration[a]

temp (°C)	pH	$E^{\circ\prime}_{I}$	$E^{\circ\prime}_{II}$	$E_{1/2}$
3	6.0	−5	−273	−5
	6.4	−14		
	6.7	−25		
	7.0	−30	−299	−34
	7.2	−38		
	7.5	−40		
	8.0	−56	−307	−64
	8.8	−79		
	9.0	−86	−319	−84
25	6.0	−24	−284	−11
	7.0	−48	−311	−32
	7.5			−58
	8.0	−81	−326	−77
	8.6			−107
	9.0	−133	−354	−134

[a] Error margins are ±5 mV for $E^{\circ\prime}_{I}$ and $E_{1/2}$ and ±10 mV for $E^{\circ\prime}_{II}$.

suggesting a e^-/H^+ transfer ratio close to 2. The small peak-to-peak separation ($\Delta E_p = E_{pa} - E_{pc}$), which increases from 5 to 25 mV over the scan rate range 10–470 mV s^{-1}, shows that the rate constant for electron exchange between the electrode and the group responsible must be quite large (Laviron, 1979b). The results of several experiments carried out at 25 °C indicate that a more complex situation develops as the temperature is raised. As evident from Figure 5B, the corresponding plot of $E^{\circ\prime}_{I}$ against pH shows some curvature. Furthermore, at pH 9, the signal I peaks appear broadened. Data are included in Table I.

The pH dependence and narrow peak shape (apart from the singular result at 25 °C and pH 9) suggest strongly that signal I corresponds to the covalently bound FAD. In so far as this group is assumed to be the immediate redox catalyst for succinate–fumarate interconversion, this proposal is supported by the observation of its complete collapse during turnover as the electrode is rotated. Previously, the FAD in fumarate reductase has been determined to have a two-electron reduction potential of −55 mV at 25 °C and pH 7 and to show a pH dependence consistent with a $2e^-/1H^+$ process (Ackrell et al., 1989). In the case of mammalian succinate dehydrogenase, potentiometric EPR measurements have shown that reduction of the FAD occurs in two consecutive one-electron steps with $E^{\circ\prime}$ values of −127 and −31 mV, respectively, at pH 7 (Ohnishi et al., 1978, 1981). The semiquinone form is therefore unstable, and $E^{\circ\prime} = -79$ mV for the effective $n = 2$ reaction. The high potential of the FAD in FRD and SDH compared to that of free flavin and other flavoenzymes is to be noted. For comparison, the reduction potential of free FAD is −210 mV at pH 7 (Clarke, 1960), while that of a histidyl-FAD peptide fragment from sarcosine dehydrogenase is −150 mV (Patek & Frisell, 1972). It is plausible that the broad redox signal in the region of −200 mV appearing at longer times and as electroactivity declines may arise from denatured forms of the enzyme in which the environment of the FAD is perturbed.

Signal II is of lower peak current amplitude and markedly broader than signal I, and the formal reduction potential shows a small dependence upon pH (see Figure 5 and Table I for data obtained at 0 and 25 °C). Several items of evidence provide support for its assignment as the $[4Fe\text{-}4S]^{2+/1+}$ cluster (center 2) in catalytically active FrdAB. The first observation is that the reduction potential, $E^{\circ\prime}_{II}$, is in the range (−285 to −320 mV) reported for center 2 on the basis of potentiometric titrations (Simpkin & Ingledew, 1985; Cammack et al., 1986; Werth et al., 1990). The second observation is that the amplitude of signal II always appears related to the size of signal I and to the corresponding catalytic activity. The third observation (to be described later) is that, under conditions of high turnover rate, the catalytic current for fumarate reduction shows a small but reproducible sigmoidal increase with an $E_{1/2}$ value that coincides with $E^{\circ\prime}_{II}$. Direct investigations of center 2 in FRD and SDH by spectroscopic methods have been problematic. The EPR spectrum of $[4Fe\text{-}4S]^{1+}$ is very broad, indicative of interaction with the paramagnetic centers 1 and 3 (Cammack et al., 1986; Maguire et al., 1985). Center 2 in succinate dehydrogenase has been characterized also by MCD spectroscopy (Johnson et al., 1985).

Signal III, which is at unusually low potential and is particularly sensitive to pH and scan rate, does not correspond to any previously measured redox process of the enzyme. At pH 8 and below, it appears as an asymmetric pair of waves which sharpen up as the scan rate or pH is lowered. We suggest that it corresponds to further proton-linked reduction of the $[3Fe\text{-}4S]^0$ cluster (center 3). Our rationale for this assignment stems from observations that we have made in voltammetric experiments on a number of smaller proteins containing [3Fe-4S] clusters. In every case thus far studied these voltammograms reveal an additional redox couple at low potential, whose wave form and effective reduction potential are also pH dependent (Armstrong et al., 1989b; Butt et al., 1991a; Iismaa et al., 1991). Furthermore, for ferredoxin III from *Desulfovibrio africanus* it was noted that the signal vanishes as the [3Fe-4S] cluster is converted into [4Fe-4S] or a heterometal analog (Butt et al., 1991a). Integrations of the low-potential signal and comparison with the charge passed for the normal $[3Fe\text{-}4S]^{1+/0}$ process led us to conclude that further reduction of $[3Fe\text{-}4S]^0$ occurs to give a novel state formally at the 2– oxidation level (Armstrong et al., 1989b). Such redox activity has not been observed for proteins containing only [2Fe-2S] or [4Fe-4S] clusters.

From reported potentiometric data for centers 1 and 3, we expect signals due to the couples $[2Fe\text{-}4S]^{2+/1+}$ and $[3Fe\text{-}4S]^{1+/0}$ to lie in the region of signal I. However, these are one-electron couples, and thus their half-height widths cannot be less than 83 mV; since the peak current for a diffusionless redox couple is proportional to n^2 (Laviron, 1979b), they should appear as broad, shallow peaks by comparison with the contribution from FAD. Considering the reported values of $E^{\circ\prime}$ for center 1 (−20 mV) and center 3 (−70 mV), they might either be extremely difficult to observe under the peaks of signal I or appear as "wings" to one or both sides of signal I, depending upon pH (Simpkin et al., 1985; Cammack et al., 1986; Werth et al., 1990). Examination of the voltammograms obtained at pH 6 and 9 does indeed provide some indication for the existence of the expected waves, respectively on the negative and positive sides of signal I.

The amount of active enzyme on the electrode surface was evaluated by three independent methods, each of which involved integration of the areas under waves or fractions of waves. Integrations were performed manually by cutting out the required sections of the voltammograms (following photocopy enlargement) and comparing their weights with a standard 'square' of known charge. For method 1, it was assumed that the clearly visible portion of signal I is dominated by a component with $n = 2$ (assigned as the FAD). Since peak current is proportional to n^2 (Laviron, 1979b), it follows that the fraction of the signal above the half-height width

Table II: Amount of Fumarate Reductase (FrdAB) Adsorbed on PGE Electrodes (pmol cm^{-2}) Evaluated by Three Independent Methods[a]

	amt of FrdAB at pH[b] (temp, °C)			
method	7 (25)	7 (0)	8 (0)	9 (0)
1	3.90	3.51	3.90	3.12
2	2.56	3.98	3.95	3.09
3	3.17	3.67	3.45	2.95

[a] See text. [b] Determinations were not carried out for pH 6 because the signals were less stable and indicated significantly smaller coverage.

effectively derives entirely from the contribution from FAD. This fraction corresponds to 25% of the total charge passed in an $n = 2$ wave envelope. Taking $\delta = 41$ and 45 mV, respectively, at 0 and 25 °C, we could thus obtain values for the number of electrochemically active FAD centers present and hence determine the number of enzyme molecules making electronic contact with the electrode. In method 2, it was assumed that the entire signal I envelope (including wings at the side) comprises couples undergoing total transfer of four electrons. In method 3, it was assumed that signal II, assigned to center 2, represents transfer of one electron per enzyme molecule. Values obtained by using methods 1, 2, and 3 are compared in Table II. Considering the different assumptions made, the results are remarkably similar, and we estimate the error to be within a factor of 25%. Taking the average of values determined for pH 7 at 25 °C (0.29 pmol) and using the electrode surface area 0.090 cm^2, we calculate the coverage Γ to be 3.2 ± 0.8 pmol cm^{-2}. Consequently, each FrdAB molecule effectively occupies an area of 5200 ± 1300 Å^2, equivalent to a square with sides of 72 ± 9 Å. Considering these dimensions and the general agreement between results obtained over a range of pH and temperature (noting particularly that Γ at 25 °C is not significantly lower than Γ determined at 0 °C), we conclude that the coverage of electroactive enzyme molecules achieved in our experiments is virtually saturative and probably close to one monolayer.

Formulation of a Basic Model for Electrocatalysis and Determination of Kinetic Parameters from RDE Experiments. The catalytic activity of adsorbed enzyme molecules for fumarate reduction was studied in some detail by RDE voltammetry, with attention focused upon the results obtained at pH 7 and 25 °C. Some experiments were also conducted for fumarate reduction at 3 °C and for succinate oxidation at 25 °C, in each case (as measured at pH 7) revealing much lower catalytic activities, while preliminary studies were carried out to assess catalysis of fumarate reduction at pH 6, 8, and 9.

Figure 6 shows a typical set of RDE voltammograms obtained for various fumarate concentrations at 25 °C and pH 7. As described earlier, it can be seen that, for low concentrations of fumarate, the transition from baseline to a constant limiting reduction current occurs within a narrow potential range as expected for a reaction that approaches the electrochemically reversible case with $n = 2$. However, as higher catalytic currents are induced, by increasing either the fumarate concentration or the rotation rate, the potential at which the current reaches i_{lim} becomes more negative. This effect appears to evolve in two stages. There is first of all a gradual negative shift in $E_{1/2}$ from the "reversible" value determined (see above) for low concentrations of fumarate or succinate, while the n value decreases. More dramatic, however, is the gross distortion that occurs as much higher catalytic currents are drawn. Under the conditions of highest enforced current, where the i–E curve appears "drawn out"

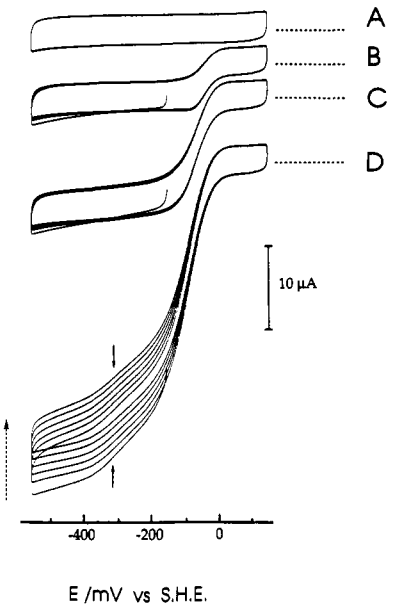

FIGURE 6: Variation of cyclic voltammetry responses at a rotating disk PGE electrode as a function of fumarate concentration. Fumarate reductase (FrdAB) 0.83 μM, polymyxin 0.2 g/L, pH 7.0 (PIPES), temperature 25 °C. Rotation rate 1200 rpm, scan rate 200 mV s^{-1}. Concentrations of fumarate are 0 μM (A), 49 μM (B), 196 μM (C), and 790 μM (D). Solid arrows indicate the position of the second wave. The broken vertical arrow indicates the decrease in activity observed for high fumarate concentration. Horizontal broken lines show the position of 0 absolute current.

toward negative potential, a second wave appears as a distinct "ripple" on the approach to i_{lim}. The $E_{1/2}$ value of this wave is –300 mV. For any particular rotation rate, i_{lim} increases with fumarate concentration to approach a maximum value. For studies with the highest levels of fumarate, e.g., 5 mM, i_{lim} becomes independent of rotation rate, including the case of a stationary electrode. At low fumarate concentration the voltammetry was found to be independent of scan rate (and thus at "steady-state") over the range 2–50 mV s^{-1}. At very high fumarate concentration, this range could be extended, for example, to at least 470 mV s^{-1} for a fumarate concentration of 4 mM. This was desirable because it was found that, with such high fumarate concentrations, activity was lost rapidly below a potential of –400 mV. It is this effect which gives rise to the decrease in catalytic current on successive cycles observed for the high-fumarate voltammogram shown in Figure 6D; at this fumarate concentration, voltammograms scanned down to a less negative potential were much more stable but were not analytically useful because the limiting current was not attained. For the high-fumarate studies, i_{lim} was thus measured on the first cycle (at –550 mV) for which the effective decrease in activity is negligible at fast scan rate (hence we employed 200 mV s^{-1} for these measurements). We have no clear explanation for the loss of activity, except for the possibility of fumarate destabilizing the enzyme layer in this potential region.

The voltammetry clearly contains a wealth of information on the electron-transport processes. In order to establish a basis for interpreting the results, it is first of all necessary to formulate a "skeleton" model which can be elaborated to account for all aspects of the observed behavior. In this paper, we shall focus upon this task by considering the system to be resolvable into three separate, independent processes as illustrated in Figure 7. Under steady-state conditions such a reaction scheme gives rise to eq 3, which is analogous to an expression giving the resultant conductance (reciprocal re-

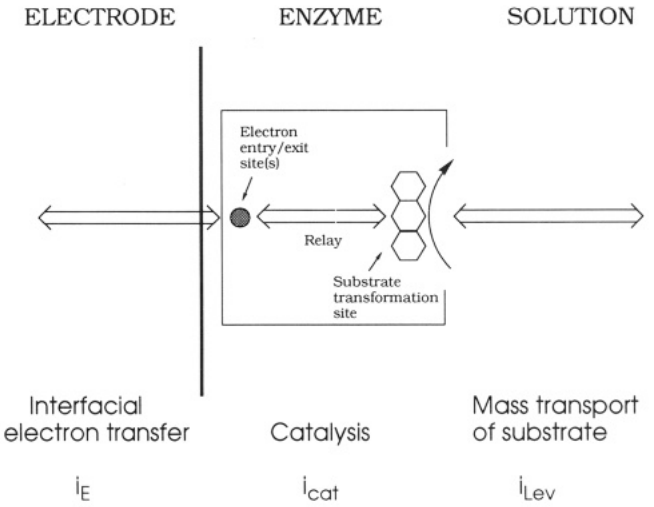

FIGURE 7: Scheme showing the sequence of steps in electron transport between electrode and substrate molecules during catalysis by an enzyme molecule adsorbed at the electrode surface.

$$1/i = 1/i_{Lev} + 1/i_E + 1/i_{cat} \quad (3)$$

sistance) of a group of resistors connected in series. The first term deals with transport of substrate molecules between the enzyme and bulk solution. This process is addressed by examining the the rotation rate dependence of the current, which for a diffusion-controlled reaction is described by the Levich equation:

$$i_{Lev} = 0.62nFAD^{2/3}C\nu^{-1/6}\omega^{1/2} \quad (4)$$

Here, A is the electrode surface area, C is the bulk concentration of substrate (mol per unit volume), D is the diffusion coefficient of substrate, ν is the kinematic viscosity of the solution (we used $\nu = 0.01$ cm^2 s^{-1} at 25 °C, a typical value for aqueous solutions), and ω is the electrode rotation rate (specifically, the angular frequency in rad s^{-1}). In the limit of an electrode reaction occurring under such conditions that it is entirely diffusion-controlled, only this term contributes and the limiting current is directly proportional to the square root of ω (Levich, 1944; Riddiford, 1965).

The second term is the "exchange current" contribution due to interfacial electron transfer between the electrode and the primary electron entry/exit site on the enzyme. In the membrane-bound complexes, the primary electron donor/acceptor site for reaction of SDH (and by analogy FRD) with Q/QH_2 is believed to be center 3 (Ohnishi et al., 1976; Beinert et al., 1977). Electrons are thus relayed between center 3 and the FAD, with center 1 probably serving as an intermediary or storage site. The question of whether this mechanism applies in the electrochemical experiment is of interest but is not addressed directly at this stage. The potential dependence of i_E is given by the current–potential characteristic shown by eq 5. This expression simplifies to the Butler–Volmer equation

$$i_E = nFAk_s[\Gamma_O \exp\{-\alpha nF(E - E^{\circ\prime})/RT\} - \Gamma_R \exp\{(1-\alpha)nF(E - E^{\circ\prime})/RT\}] \quad (5)$$

for diffusing redox couples under conditions in which the bulk substrate concentration equals that at the electrode surface (Laviron 1979; Bard & Faulkner, 1980; Bond, 1980; Southampton Electrochemistry Group, 1985). Here, Γ_O and Γ_R are the respective surface concentrations of the oxidized and the reduced form of the enzyme (expressed as mol per unit surface area), α is the transfer coefficient, n is the number of electrons transferred in the transition state, E is the applied electrode potential, and $E^{\circ\prime}$ is the appropriate apparent standard reduction potential of the system. The *standard* first-order rate constant, k_s (the *exchange* rate constant), reflects the ease of moving electrons between the electrode and the enzyme. At applied potentials much more positive or negative than $E^{\circ\prime}$, only oxidation *or* reduction components (respectively) become significant. Equation 6 shows how the

$$|i_E| = nFA\Gamma k_E \quad (6)$$

potential-dependent terms i_E and k_E (the first-order electrochemical rate constant) are interrelated. The quantity Γ is the total number of enzyme molecules adsorbed per unit area of electrode and thus equals $\Gamma_O + \Gamma_R$.

The third term of eq 3 describes the intrinsic catalytic properties of the enzyme in its reaction with substrate and is assumed to be independent of driving force and electrode rotation rate. It can be expressed as an electrochemical form of the Michaelis–Menten expression as given in eq 7. The

$$i_{cat} = nFA\Gamma k_{cat}C/(C + K_M) \quad (7)$$

quantities K_M and k_{cat} are the apparent Michaelis–Menten parameters, which are assumed to be independent of applied potential. In the limit of $C \gg K_M$, i_{cat} becomes independent of C.

Equations 3–7 predict an interrelationship between current, applied potential, substrate concentration, and electrode rotation rate. For a wide range of experimental conditions, further analysis can be facilitated by removing from consideration the influence of electrochemical driving force (and thus k_E). We note from eq 3 that the term $1/i_E$ vanishes under the condition $i_E \gg i_{cat}$ and i_{Lev}, which is favored by the intrinsic quantities k_s (large), k_{cat} (small), and K_M (large) and by the experimental variables decreasing C (eqs 4 and 7), decreasing ω (eq 4), and sufficiently large values of the electrochemical driving force, $|E - E^{\circ\prime}|$ (eq. 5). In the resulting i–E profile, the current reaches a constant value, i_{lim} once the electrochemical driving force ceases to be a controlling factor.

We measured i_{lim} as a function of $\omega^{1/2}$ for a range of fumarate concentrations at 25 °C and analyzed data according to eq 4. Results of four experiments are shown in Figure 8A. The nonlinear appearance of the Levich plots show that as ω is increased, the current is determined increasingly by the rate of catalysis as opposed to mass transport. Combining eqs 3, 4, and 7 yields a form of the Koutecky–Levich equation (eq 8), which describes the variation of $1/i_{lim}$ with $\omega^{-1/2}$ for different

$$1/i_{lim} = (C + K_M)/(nFA\Gamma k_{cat}C) + 1/(0.62nFAD^{2/3}C\nu^{-1/6}\omega^{1/2}) \quad (8)$$

values of C. The corresponding plot of $1/i_{lim}$ against $\omega^{-1/2}$ is shown in Figure 8B. The intercept on the $1/i_{lim}$ axis (the reciprocal current extrapolated to infinite rotation rate) is now identified with $1/i_{cat}$ (eq 7). Analysis of the resultant slopes from the Koutecky–Levich plots gave a value of D for fumarate of 1.1×10^{-5} cm^2 s^{-1}, using $n = 2$.

In Figure 8C we have plotted the resulting values of i_{cat}/A (catalytic current density) against C. As the substrate concentration is increased, i_{cat}/A approaches a limiting value, i_{max}/A. At low C values the limiting slope is 2.56 ± 0.01 A cm^{-2} M^{-1} (M^{-1} = per mol fumarate per liter). Inserting numerical values, including $\Gamma = 3.2 \times 10^{-12}$ mol cm^{-2} determined as described earlier, we obtain the value 5.3×10^6 M^{-1} s^{-1} for the second-order rate constant (k_{cat}/K_M) for fumarate reduction by the enzyme. Expressed in the familar

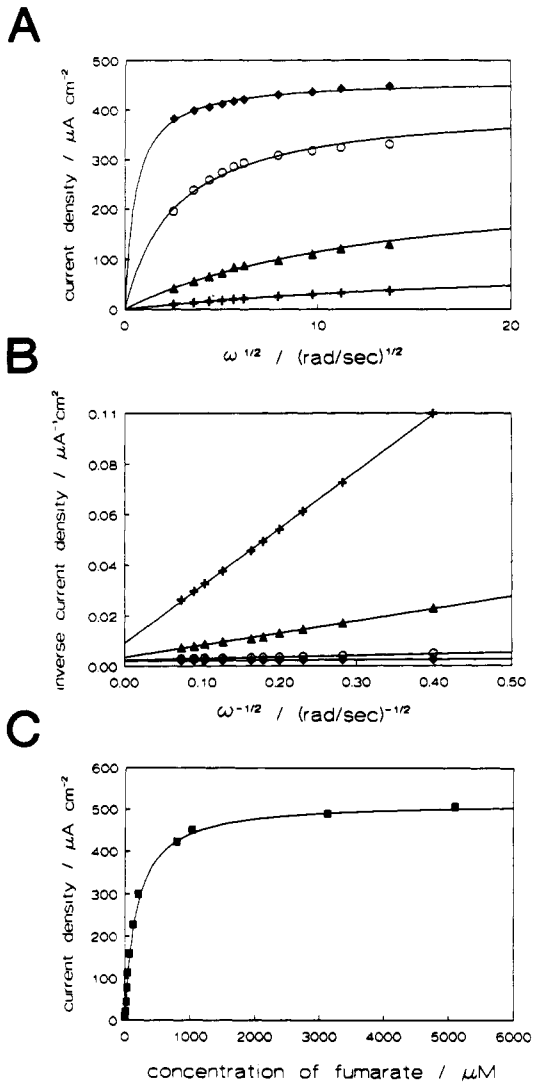

FIGURE 8: (A) Levich plot for reduction of fumarate by fumarate reductase adsorbed at a PGE electrode (see text for explanation): temperature, 25 °C; 0.7 μM FrdAB; 0.1–0.2 g/L polymyxin; pH 7.0 (PIPES). Fumarate concentrations are 40 μM (+), 200 μM (▲), 1.0 mM (○), and 5.0 mM (◆). (B) Koutecky–Levich plot of data used in (A). (C) Dependence of catalytic current density (i_{cat}/A) upon fumarate concentration: temperature, 25.0 °C; pH 7.0 (PIPES); 0.1 or 0.2 g/L polymyxin; 0.8 μM FrdAB. The line shown is the nonlinear regression fit giving K_M = 161 ● 7 μM, and i_{max}/A = 520 μA cm^{-2} (thus k_{cat} = 840 s^{-1}).

formalism of enzyme kinetic theory, the terms i_{max}/nF and $A\Gamma k_{cat}$ each represent the electrochemical analog of V_{max}. Proceeding further, by independently fitting the data shown in Figure 8C to the Michaelis–Menten model (eq 7), we obtain the values k_{cat} = 840 ± 13 s^{-1} and K_M = 161 ± 7 μM. The errors given arise in the data analysis, and the rate constants do not reflect the estimated 25% uncertainty in Γ.

Comparisons can be made with results from nonelectrochemical assays using benzyl viologen as electron donor. Apparent K_M values of 410–470 μM have been obtained for Triton-solubilized and membrane-bound preparations of fumarate reductase at room temperature and pH 7 (Dickie & Weiner, 1979). From the specific activity assay with benzyl viologen (511 units mg^{-1}) we calculate the equivalent k_{cat} value to be 396 s^{-1}. At 38 °C, fumarate reductase gives k_{cat} values of ca. 1000 s^{-1} (Ackrell et al., 1992). Thus, when viewed electrochemically, FRD is at least as active as it appears from traditional methods.

We now consider the likely cause of the asymmetric distortion of the voltammograms obtained under conditions of high current (high C, high ω). Much of this may be attributed to the increasing influence of the potential-dependent term i_E in eq 3. We determined (see above) that the catalytic activity of adsorbed FrdAB is extremely high. The apparent retardation thus arises from the limitation that originates in the potential-dependent current term, i_E (eq 5), and, through eq 6, in the electrochemical rate constant, k_E, for interfacial electron transfer between electrode and electron entry/exit site in the enzyme. Under conditions whereby turnover is limited by the rate of arrival of substrate (as favored by low substrate concentration and low rotation rate), an adequate rate of electron transfer to the enzyme is achieved without the need for an elevated driving force. In this case the electrochemical reaction approaches reversibility. However, an increase in the substrate concentration or the rotation rate stimulates a higher demand for electrons. The system now becomes sensitive to factors that will increase i_E and therefore responds to the electrochemical driving force. We thus expect distortion of the i–E profile, as is indeed observed.

Two comments can be made about rates of electron transfer in this system. First, the observation that the distortion is only severe at high currents illustrates how conductive a contact the enzyme makes with the electrode. From the small value of the peak separation, ΔE_p, observed for signal I at scan rates up to 470 mV s^{-1}, we can estimate a lower limit for k_s using the treatment described by Laviron (1979b). This is of the order of 100 s^{-1}, which is sufficiently large to ensure an adequate supply of electrons at low substrate levels (thus the electrochemistry appears to approach reversibility) but certain to be restrictive once demand is increased. Second, the large k_{cat} value requires that any intramolecular electron-relay process must be very fast, i.e., with a rate constant at least of the order of 1600 s^{-1} for a single pathway.

With this reasoning, we can now propose an explanation for the second sigmoidal wave that appears in rotating-disk voltammograms at high substrate concentration. The position of this wave coincides with the formal reduction potential, $E^{\circ\prime}_{II}$, of signal II which we have tentatively assigned to center 2. If the [4Fe-4S] cluster is also capable of functioning as an electron entry site on the enzyme, then a second pathway should become available to relay electrons from the electrode to the FAD. This could be utilized in parallel with the primary pathway, boosting the supply and thus increasing the catalytic current. Participation of this auxilliary electron entry site would be detectable under conditions where substrate turnover is limited by the rate of supply of electrons and should become effective as the applied potential approaches its formal reduction potential, $E^{\circ\prime}_{II}$. These features are indeed observed; the small "boost" results in the current reaching i_{lim} (in this case almost at the level of i_{max}) at a potential more positive than would otherwise be the case.

Experiments conducted for fumarate reduction (pH 7) at 3 °C showed similar evidence for fast interfacial electron transfer, but values of i_{lim} were much smaller, and Levich plots displayed appreciable curvature even for low concentrations of fumarate. An analysis of data according to the above procedure gave k_{cat} = 14 s^{-1} and K_M = 33 μM. These results show a large temperature coefficient for the kinetics and suggest that the enzyme's intrinsic catalytic properties play a greater part in determining the rate as the temperature is lowered.

A limited amount of data were obtained for succinate dehydrogenation over the concentration range 0–600 μM at pH 7 and 25 °C. Catalytic currents were much smaller than observed for fumarate reduction under the same conditions;

indeed we noted that even trace amounts of fumarate present in the succinate solution produced a reduction current which interfered with measurements. Sigmoidal i–E profiles were obtained with values of i_{lim} that were independent of electrode rotation rate over the range 0–1800 rpm. Evidently, for catalysis of succinate oxidation, the catalytic term (eq 7) is the sole rate-determining factor under these conditions.

Additionally, preliminary studies were carried out to assess the pH dependence of fumarate reduction at 3 and 25 °C. We restricted our experiments to low fumarate concentrations, noting the position of the catalytic $E_{1/2}$ value and the magnitude of catalytic currents. Two general effects were noted as the pH was increased from 6 to 9: catalytic currents decreased, and $E_{1/2}$ values became more negative. In no case could we detect any evidence for a potential-dependent activity switch-off as observed for SDH (Sucheta et al., 1992). Thus an important difference exists between the two enzymes, perhaps the result of evolutionary changes that have altered the order or relative rates of internal catalytic events.

Data for $E_{1/2}$ are listed in Table I and displayed in Figure 5. For the low-temperature studies, the correspondence between $E^{\circ\prime}{}_1$ and $E_{1/2}$ is extremely close and implicates the two-electron reduced form of FAD as a key intermediate in the catalytic reaction. However, at higher temperature, a different pattern of behavior is found, in that $E_{1/2}$ varies linearly with pH (slope –49 mV) and *precedes* $E^{\circ\prime}{}_1$ for pH values of 7 and below. Subtle aspects of a complicated electron-transport reaction are thus immediately in evidence. We believe that these results reveal a shift in the rate-determining step; for example, a bond-breaking process (large $\Delta H^{\ddagger}$) which occurs at the active site (and which controls the rate at low temperature) could give way to an intramolecular electron-transfer step (small $\Delta H^{\ddagger}$) as the temperature is increased. Although we have not made a detailed study of the effect of temperature on rates, the large decrease in k_{cat} observed upon lowering the temperature from 25 to 3 °C provides independent evidence for the presence of a high-$\Delta H^{\ddagger}$ step in the catalytic reaction. Further studies are required in order to formulate an interpretation of the variation of $E_{1/2}$ and n values observed under different conditions.

The results that we have presented now demonstrate the feasibility of conducting an in-depth analysis of a complex electron-transport enzyme using voltammetric methods. Dynamic electrochemistry exploiting rapid, direct electron exchange with redox centers in an enzyme that is attached to the electrode offers a unique way to address the various components of catalysis. The approach provides exquisite capabilities for precise control of important reaction variables (particularly potential control, driving force, and mass transport) and for viewing active-site redox transformations and revealing their participation in turnover. By such means we should be able to examine the intricate relationships between overall driving force and internal energetics. Fumarate reductase and succinate dehydrogenase can now be recognized as excellent subjects for electrochemical studies of enzymatic electron-transport systems.

ACKNOWLEDGMENT

We are grateful to Julea Butt, who conducted preliminary electrochemical experiments with fumarate reductase.

REFERENCES

Ackrell, B. A. C., Cochran, B., & Cecchini, G. (1989) *Arch. Biochem. Biophys. 268,* 26–34.

Ackrell, B. A. C., Johnson, M. K., Gunsalus, R. P., & Cecchini, G. (1992) in *Chemistry and Biochemistry of Flavoenzymes* (Mueller, F., Ed.) Vol. 3, pp 229–297, CRC Press, Boca Raton, FL.

Ackrell, B. A. C., Armstrong, F. A., Sucheta, A., & Yu, T. (1993) (submitted for publication).

Adams, R. N (1969) *Electrochemistry at Solid Electrodes,* Marcel Dekker, New York.

Armstrong, F. A. (1990) *Struct. Bonding 72,* 137–221.

Armstrong, F. A. (1992) in *Advances in Inorganic Chemistry 38,* (Sykes, A. G., & Cammack, R., Eds.) pp 117–163, Academic Press, New York.

Armstrong, F. A., & Lannon, A. M. (1987) *J. Am. Chem. Soc. 109,* 7211–7212.

Armstrong, F. A., George, S. J., Cammack, R., Hatchikian, E. C., & Thomson, A. J. (1989a) *Biochem. J. 264,* 265–273.

Armstrong, F. A., Butt, J. N., George, S. J., Hatchikian, E. C., & Thomson, A. J. (1989b) *FEBS Lett. 259, 15–18.*

Armstrong, F. A., Butt, J. N., & Sucheta, A. (1993a) *Methods Enzymol.* (in press).

Armstrong, F. A., Bond, A. M., Büchi, F. N., Hamnett, A., Hill, H. A. O., Lannon, A. M., Lettington, O. C., & Zoski, C. G. (1993b) *Analyst* (in press).

Bard, A. J., & Faulkner, L. R. (1980) *Electrochemical Methods. Fundamentals and Applications,* Wiley, New York.

Beinert, H., Ackrell, B. A. C., Vinogradov, A. D., Kearney, E. B., & Singer, T. P. (1977) *Arch. Biochem. Biophys. 182,* 95–106.

Blaut, M., Whittaker, K., Valdovinos, A., Ackrell, B. A. C., Gunsalus, R. P., & Cecchini, G. (1989) *J. Biol. Chem. 264,* 13599–13604.

Bond, A. M. (1980) *Modern Polarographic Methods in Analytical Chemistry,* Marcel Dekker, New York.

Butt, J. N., Armstrong, F. A., Breton, J., George, S. J., Thomson, A. J., & Hatchikian, E. C. (1991a) *J. Am. Chem. Soc. 113,* 6663–6670.

Butt, J. N., Sucheta, A., Armstrong, F. A., Breton, J., Thomson, A. J., & Hatchikian, E. C. (1991b) *J. Am. Chem. Soc. 113,* 8948–8950.

Butt, J. N., Sucheta, A., Armstrong, F. A., Breton, J., Thomson, A. J., & Hatchikian, E. C. (1993) *J. Am. Chem. Soc. 115,* 1415–1421.

Cammack, R., Patil, D. S., Condon, C., Owen, P., Cole, S. T., & Weiner, J. H. (1984) in *Flavins and Flavoproteins* (Bray, R. C., Engel, P. C., & Mayhew, S. G., Eds.) pp 551–554, Walter de Gruyter, New York.

Cammack, R., Patil, D. S., & Weiner, J. H. (1986) *Biochim. Biophys. Acta 870,* 545–551.

Cammack, R., Maguire, J. J., & Ackrell, B. A. C. (1987) in *Cytochrome Systems; Molecular Biology and Bioenergetics* (Papa, S., Chance, B., & Ernster, L., Eds.) p 485, Plenum, New York.

Clark, W. M. (1961) *Oxidation–reduction Potentials of Organic Systems,* Williams and Wilkins, Baltimore.

Cole, S. T., Condon, C., Lemire, B. D., & Weiner, J. H. (1985) *Biochim. Biophys. Acta 811,* 381–403.

Dickie, P., & Weiner, J. H. (1979) *Can. J. Biochem. 57,* 813–821.

Haddock, B. A., & Jones, C. W. (1977) *Bacteriol. Rev. 41,* 47–99.

Hayashi, K., & Suzuki, T. (1965) *Bulletin Inst. Chem. Res., Kyoto Univ. 43,* 259–277.

Heyrovský, J., & Kůta, J. (1966) *Principles of Polarography,* Academic Press, New York.

Hill, H. A. O. (1993) *Methods Enzymol.* (in press).

Iismaa, S. E., Vazquez, A. E., Jensen, G. M., Stephens, P. J., Butt, J. N., Armstrong, F. A., & Burgess, B. K., (1991) *J. Biol. Chem. 266,* 21563–21571.

Ingledew, W. J., & Poole, R. K. (1984) *Microbiol. Rev. 48,* 222–271.

Johnson, M. K., Morningstar, J. E., Bennett, D. E., Ackrell, B. A. C., & Kearney, E. B. (1985) *J. Biol. Chem. 260,* 7368–7378.

Laviron, E. (1979a) *J. Electroanal. Chem. Interfacial Electrochem. 100,* 263–270.

Laviron, E. (1979b) *J. Electroanal. Chem. Interfacial Electrochem. 101,* 19–28.

Lemire, B. D., & Weiner, J. H. (1986) *Methods Enzymol. 126,* 377–386.

Levich, V. G. (1944) *Acta Physicochim. URSS 19,* 117–132.

Maguire, J. J., Johnson, M. K., Morningstar, J. E., Ackrell, B. A. C., & Kearney, E. B., (1985) *J. Biol. Chem. 260,* 10909–10912.

Manodori, A., Cecchini, G., Schröder, I., Gunsalus, R. P., Werth, M. T., & Johnson, M. K. (1992) *Biochemistry 31,* 2703–2712.

Nicholson, R. S. & Shain, I. (1964) *Anal. Chem. 36,* 706–723.

Ohnishi, T. (1987) *Curr. Top. Bioenerg. 15,* 37–65.

Ohnishi, T., Salerno, J. C., Maida, T., Yu, C. A., Nagaoka, S., & King, T. E. (1978) in *Frontiers of Biological Energetics* (Dutton, P. L., Leigh, J. S., & Scarpa, A., Eds.) pp 165–173, Academic Press, New York.

Ohnishi, T., King, T. E., Salerno, J. C., Blum, H., Bowyer, J. R., & Maida, T. (1981) *J. Biol. Chem. 256,* 5577–5582.

Patek, D. R., & Frisell, W. R. (1972) *Arch. Biochem. Biophys. 150,* 347–354.

Riddiford, A. C. (1965) *Adv. Electrochem. Electrochem. Eng. 4,* 47–97.

Robinson, J. J., & Weiner, J. H. (1982) *Can. J. Biochem. 60,* 811–816.

Schröder, I., Gunsalus, R. P., Ackrell, B. A. C., Cochran, B., & Cecchini, G. (1991) *J. Biol. Chem. 266,* 13572–13579.

Simpkin, D., & Ingledew, W. J. (1985) *Biochem. Soc. Trans. 13,* 603–607.

Southampton Electrochemistry Group (1985) *Instrumental Methods in Electrochemistry,* Ellis Horwood series in Physical Chemistry,) Ellis Horwood, Chichester.

Sucheta, A., Ackrell, B. A. C., Cochran, B., & Armstrong, F. A. (1992) *Nature 356,* 362–363.

Varfolomeev, S. D., & Berezin, I. V. (1978) *J. Mol. Catal. 4,* 387–399.

Weiner, J. H., & Dickie, P. (1979) *J. Biol. Chem. 254,* 8590–8593.

Weiner, J. H., Cammack, R., Cole, S. T., Condon, C., Honore, N., Lemire, B. D., & Shaw, G. (1986) *Proc. Natl. Acad. Sci. U.S.A. 83,* 2056–2060.

Werth, M. T., Cecchini, G., Manodori, A., Ackrell, B. A. C., Schröder, I., Gunsalus, R. P., & Johnson, M. K. (1990) *Proc. Natl. Acad. Sci. U.S.A. 87,* 8965–8969.

Werth, M. T., Sices, H., Cecchini, G., Schröder, I., Lasage, S., Gunsalus, R. P., & Johnson, M. K. (1992) *FEBS Lett. 299,* 1–4.

Westenberg, D. J., Gunsalus, R. P., Ackrell, B. A. C., & Cecchini, G. (1990) *J. Biol. Chem. 265,* 19560–19567.